Mutations in the S4–H2 loop of eIF4E which increase the affinity for m^{7}GTP

Taly Spivak-Kroizman[a], Diana E. Friedland[b], Christine De Staercke[a], Kim M. Gernert[c], Dixie J. Goss[b], Curt H. Hagedorn[a,*]

[a] *Departments of Medicine, Genetics Program of the Winship Cancer Center, and the Program for Biochemistry, Cell, and Developmental Biology, Emory University School of Medicine, 165 Michael Street, Room 201, Atlanta, GA 30322, USA*
[b] *Department of Chemistry, Hunter College of the City University of New York, New York, NY 10021, USA*
[c] *Biomolecular Computing Resource and Department of Biochemistry, Emory University School of Medicine, Atlanta, GA 30322, USA*

Received 10 January 2002; revised 8 February 2002; accepted 8 February 2002

First published online 26 February 2002

Edited by Thomas L. James

Abstract Eukaryotic initiation factor 4E (eIF4E) binds the 5′-cap of eukaryotic mRNAs and overexpression of eIF4E in epithelial cell cancers correlates with the metastases/tissue invasion phenotype. Photolabeling of eIF4E with [γ-^{32}P]8-azidoguanosine 5′-triphosphate (8-N_3GTP) demonstrated cross-linking at Lys-119 in the S4–H2 loop which is distant from the m^{7}GTP binding site [Marcotrigiano et al. (1997) Cell 89, 951–961; Friedland et al. (1997) Protein Sci. 6, 125–131]. Modeling studies indicate that 8-N_3GTP cross-linked with Lys-119 because it binds a site that is occupied by the second nucleotide of a bound mRNA. Mutagenesis of the S4–H2 loop produced proteins with a 5–10-fold higher affinity for m^{7}GTP than wild-type eIF4E. These mutants of eIF4E may have uses in selectively purifying mRNAs with intact 5′-ends or in determining how the promyelocytic leukemia protein decreases the affinity of eIF4E for mRNA caps.

Key words: RNA binding protein; Eukaryotic initiation factor 4E; mRNA cap; m^{7}GTP; Translation

1. Introduction

Regulation of gene expression at the level of translation occurs in many biological processes including cell growth and differentiation, embryonic development, and viral infection. Evidence is accumulating that perturbations in mRNA translational elements play a major role in the biology of some cancers [3–7]. In addition, at least one small molecule anti-cancer agent is believed to exert its effect by inhibiting initiation of mRNA translation [8]. A critical protein mediating early events in initiation of translation is the eukaryotic initiation factor 4E (eIF4E). eIF4E serves as an intermediary between the 5′-cap (m^{7}G(5′)ppp(5′)N), several other initiation factors plus the poly(A) binding protein (PAB), and the 3′-poly(A) tail of eukaryotic mRNA [9,10]. It has a binding site for m^{7}GDP on one side and a binding site for eukaryotic initiation factor 4G (eIF4G) (or PHAS-I) on the other side of its central β-sheet [1,11,12]. eIF4E is part of the eIF4F complex that includes eIF4G, which binds ribosomes and PAB, and eIF4A, which is an ATP-dependent RNA helicase [13]. The binding of eIF4F and eIF4B to the mRNA cap appears to be a key step in the ATP-dependent unwinding of mRNA structure and ribosome binding which are rate limiting events for the translational initiation of many eukaryotic mRNAs [14].

eIF4E and assembly of the eIF4F complex are targets of regulation during the stimulation of cell growth and differentiation [15–17]. In addition, overexpression or microinjection of eIF4E causes malignant transformation in NIH 3T3 cells and aberrant growth in HeLa cells [18,19]. Elevated levels of eIF4E mRNA and protein are found in a variety of epithelial cell cancers [3,5]. The binding of eIF4E to eIF4G is regulated by interactions with translational repressor proteins which sequester eIF4E for release under selected physiological conditions [20,21]. On the other hand, eIF4E- and eIF4E-associated proteins are targeted during growth inhibitory events. For example, during apoptosis at least one eIF4E-associated protein is targeted for proteolytic destruction [22]. In addition, the promyelocytic leukemia protein (PML) which inhibits cell transformation and growth has recently been shown to bind eIF4E and decrease the affinity for mRNA caps [23,24].

The structure of a cocrystal of mammalian eIF4E bound to m^{7}GDP and the structure of yeast eIF4E bound to m^{7}GDP in solution have been solved [1,11,12]. Both studies describe a cap binding slot for eIF4E in which the m^{7}G moiety is sandwiched between the side chains of two tryptophans, Trp-56/Trp-102 in mammalian and Trp-58/Trp-104 in yeast eIF4E. Mutagenesis studies of the m^{7}GDP binding site of eIF4E support the hypothesized π–π stacking that occurs between the m^{7}G moiety and the two tryptophan residues [25]. In addition, several residues interact with m^{7}G by hydrogen bonding. These include Trp-166 in mammalian and yeast, as well as Glu-103 in mammalian, and Glu-105 in yeast eIF4E which form hydrogen bonds with m^{7}G [1,11].

The results of specific photoaffinity labeling of recombinant mammalian eIF4E with [γ-^{32}P]8-azidoguanosine 5′-triphosphate (8-N_3GTP) suggested that residues near Lys-119, the site of photoinsertion, interacted with this nucleotide probe [2]. We report a molecular model built with the coordinates of eIF4E/m^{7}GDP cocrystal structure and its use to identify

*Corresponding author. Fax: (1)-404-712-2980.
E-mail address: chagedo@emory.edu (C.H. Hagedorn).

Abbreviations: eIF4E, eukaryotic initiation factor 4E; eIF4G, eukaryotic initiation factor 4G, also called p220 or eIF4γ; PHAS-I, phosphorylated heat- and acid-stable protein regulated by insulin, also called 4E binding protein 1 (4E-BP1); 8-N_3GTP, 8-azidoguanosine 5′-triphosphate

0014-5793/02/$22.00
PII: S0014-5793(02)02445-6

possible binding sites for the [γ-^{32}P]8-N_3GTP probe on the surface of eIF4E near the S4–H2 (N118–Q120) loop. The site of cross-linking of the nucleotide probe, the S4–H2 loop, was analyzed by mutagenizing residues Asn-118 through Gln-121 to alanine and determining the effect on 4E functions.

2. Materials and methods

2.1. Modeling of the capped mRNA binding site of eIF4E

The eIF4E structure was studied to determine the possible binding site of [γ-^{32}P]8-N_3GTP ([1,2], PDB ID# 1EJ1, 1EJ4, 1EJH). The program DOCK was run on the apo-protein structure (eIF4E without m^7GDP present) to locate potential mRNA binding sites on the protein surface [25]. First, cavities were located on the protein surface by probing with a sphere equivalent to H_2O (1.4 Å). A cavity is defined by a cluster of spheres which are in contact and are complementary to a pocket in the molecular surface of the protein. More than 20 cavities were located on the surface of eIF4E. Three interconnected cavities localized near the site of m^7GDP in the cocrystal structure were searched for nucleotide binding sites. When searched with m^7GDP as the ligand, DOCK located a m^7GDP binding site within 1.5 Å of the m^7GDP bound in the cocrystal structure. Next GMP was used as the ligand to search for other possible mRNA binding sites because it is a single repeating unit of RNA. An atomic match of GMP to a subset of spheres within a cavity defined a potential nucleotide binding site. All potential GMP binding sites were located and sorted to identify those which positioned the ribose and phosphate of the base in an appropriate orientation to form growing RNA chains of three nucleotides from a m^7GDP moiety which was fixed as in the cocrystal structure [1]. Two initial mRNA conformations formed using this approach were submitted as ligands in flexible docking runs onto the apo-eIF4E structure using SYBYL FlexiDock [26]. The m^7GDP cap was held fixed within the determined binding site, the protein molecule was held fixed, and the remainder of the RNA tail was allowed to flex and rotate. These studies formed the basis for the hypothesized location of an mRNA bound to eIF4E.

2.2. Mutagenesis of eIF4E

Wild-type $eIF4E_{human}$ in a pET-3d vector was used as a template for QuikChange™ PCR-based site-directed mutagenesis (Stratagene) [25,27]. Mutagenesis primer oligonucleotides were designed to introduce alanine substitutions at residues N118, K119, Q120, and Q121, and used according to the instructions provided by the manufacturer. All plasmids were sequenced (both strands of the eIF4E coding region) to confirm mutagenesis. The nomenclature of mutants indicates the substituted amino acid, its position, and the replacing residue (e.g. lysine at position 119 replaced by alanine is designated K119A).

2.3. Expression and purification of eIF4E mutants and PHAS-I

Escherichia coli BL21(DE3) expressing wild-type or mutants of $eIF4E_{human}$ were grown at 37°C in M9ZB media containing ampicillin. Cells were induced at an OD_{600} of 0.6 with 0.4 mM IPTG and incubated for an additional 3 h. Wild-type and mutant proteins were purified from these cultures as previously described [27]. PHAS-I was expressed and purified as described elsewhere [28]. The PHAS-I expression vector and rabbit anti-PHAS-I antibodies were kindly provided by Dr. J.C. Lawrence [28].

2.4. Circular dichroism measurements

Circular dichroism spectra of FPLC-purified eIF4E proteins were measured on a Jasco-J710 spectropolarimeter [29,30]. Spectra were obtained in a 0.1 M phosphate buffer at pH 7.6. All measurements were performed using a 0.5 mm pathlength quartz cell at 25°C. Each sample was scanned 10 times and high frequency noise reduction was applied. Data were recorded at 0.5 mm intervals with a time constant of 1.0 s and a 1.0 nm constant spectral bandwidth.

2.5. Fluorescence measurements of the K_d of eIF4E for m^7GTP

Fluorescence titration experiments were performed to determine the K_d of m^7GTP binding to wild-type and mutant eIF4E. The buffer used for all fluorescence measurements was 20 mM HEPES-KOH (pH 7.6) and 1 mM dithiothreitol (DTT). Measurements were performed at 25°C on a SPEX Fluorolog-T2 spectrofluorometer equipped with a high intensity (450 W) xenon arc lamp. An excitation wavelength of 289 nm was used to monitor the tryptophan fluorescence emission of the proteins. Excitation and emission slit widths of 1.5 and 2.0 mm, respectively, were used and a 1.0 cm sample cell path length was employed. The steady state data were collected and analyzed as described previously [29,31].

3. Results and discussion

3.1. Modeling studies of 8-N_3GTP binding to eIF4E

Previous studies have shown that an 8-N_3GTP photoprobe specifically bound to mammalian eIF4E and that the site of cross-linking was Lys-119 [2]. Modeling studies were done with the coordinates of the eIF4E/m^7GDP cocrystal to identify the most likely surface cavity that bound the 8-N_3GTP probe. They demonstrated that it was highly improbable that the photoprobe bound to the m^7GDP binding site in the cocrystal structure [1]. In the eIF4E/m^7GDP cocrystal structure the m^7GDP binding site covers the edge of the central β-sheet (strands 1, 3, and 5) [1]. Lys-119 is at the end of strand 4 which is two strands away from the m^7GDP binding site at a distance of approximately 19–20 Å. The side chain of Lys-119 could not extend this distance in the model to interact with 8-N_3GTP in the m^7GDP binding site (between Trp-56 and Trp-102), and since Lys-119 is one residue off the end of a β-strand in the center of the sheet, the backbone surrounding position 119 could not extend to allow this interaction. Moreover, other lysine residues that were on flexible loop structures line the m^7GDP binding site (Lys-49, Lys-52, and Lys-54 in the 1–2 loop and Lys-106 in the 3–4 loop) and were more likely candidates to cross-link with 8-N_3GTP bound in the m^7GDP binding site [1]. Based on the modeling studies we conclude that 8-N_3GTP did not bind eIF4E in the m^7GDP site formed by the S1–S2 and S3–S4 loops.

If the 8-N_3GTP photoprobe did not bind in the m^7GDP binding site then what site on eIF4E would specifically bind this nucleotide? Modeling suggests that in order to interact with Lys-119, the 8-N_3GTP probe bound to sites that we hypothesize bind the second and third nucleotides of a bound mRNA (Fig. 1B). GMP was used as the ligand to probe the apo-protein structure of eIF4E with the program DOCK (see

→

Fig. 1. Model of GMP binding sites and m^7GpppGGG bound to eIF4E. In both A and B the structure of wild-type eIF4E is displayed as a ribbon. The β-strands are colored yellow and labeled as previously defined [1]. The S4–H2 loop (extending from strand 4; residues 118–121) is colored red. The positions of side chains of Lys-159 and Ser-209 are labeled in white. Lys-119 was modeled, labeled and displayed (capped sticks, represented by atom color with carbons being green). A: A refined set of binding sites for GMP as identified by DOCK (see Section 2). The m^7Gpp present in the eIF4E/m^7GDP cocrystal structure is shown in space fill. Only GMP molecules which orient the ribose and phosphate in the 5′ to 3′ direction toward the m^7G cap are shown. Note that two different potential binding sites for the fourth nucleotide are shown (lower left of the panel). B: The preferred mRNA position, as determined by modeling, is shown. The m^7Gpp present in the eIF4E/m^7GDP cocrystal structure is shown in space fill. The second, third, and fourth nucleotides of the modeled mRNA (m^7GpppGGG) are shown in magenta. The location of this modeled mRNA binding site is consistent with the proposed path of a capped mRNA [1], and the solution structure of yeast eIF4E with bound m^7GpppA [11]. The second nucleotide binds between Ser-209 and Lys-159, while the third and fourth nucleotides pack along the edge of the cavity demarcated by Lys-159 and Lys-119.

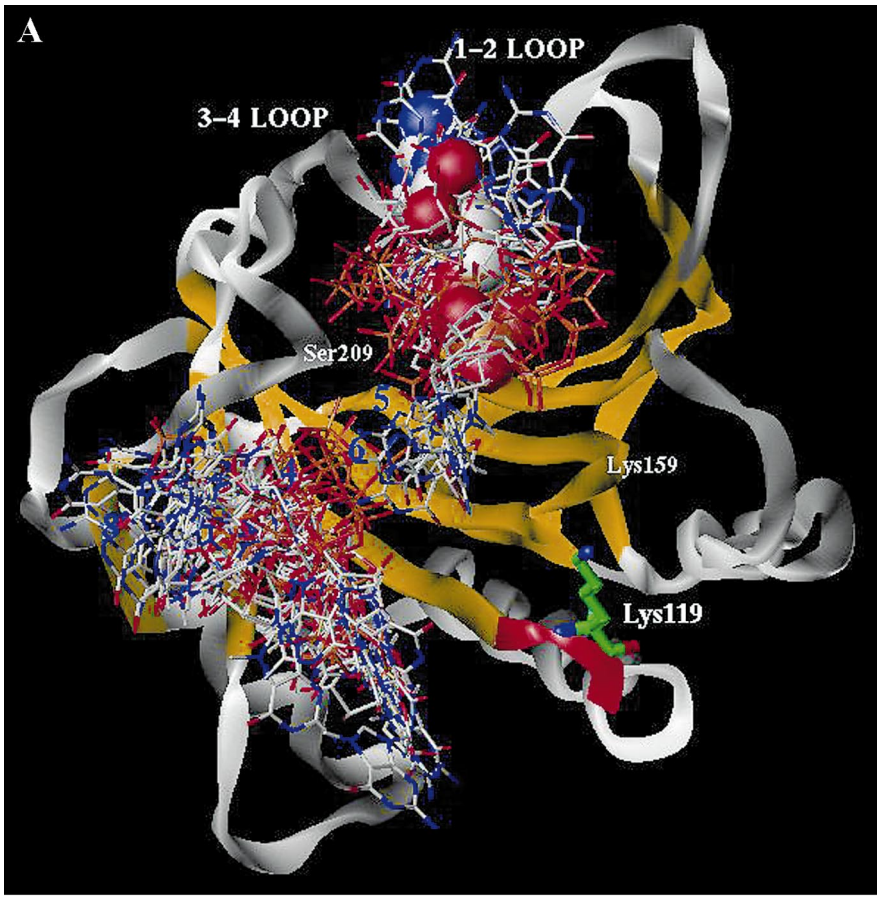
A
1–2 LOOP
3–4 LOOP
Ser209
5
6
Lys159
Lys119

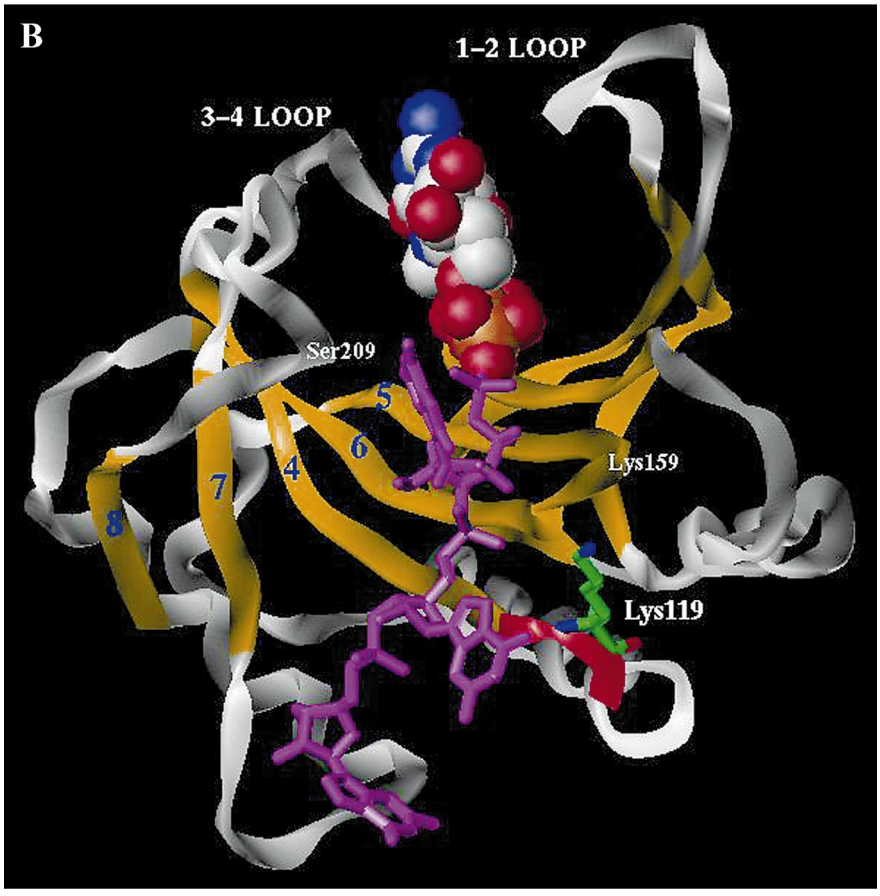
B
1–2 LOOP
3–4 LOOP
Ser209
5
6
4
7
8
Lys159
Lys119

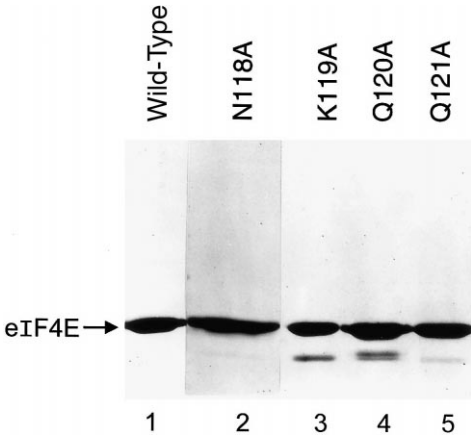

Fig. 2. Purification of eIF4E mutants. Expression and purification of all mutants of eIF4E was performed as described in Section 2. The recombinant proteins recovered from the final FPLC purification step were analyzed by 12% SDS–PAGE. A Coomassie blue-stained gel with 30 μg of each eIF4E mutant is shown.

Section 2) and the binding sites were clustered within the predicted path of an mRNA [1] (Fig. 1A). The bound GMP molecules were then linked to form RNA chains (m^7GpppGGG) and minimized using FlexiDock. The predicted mRNA conformations packed in one of two binding channels. The 5′-m^7Gpp moiety and second nucleotide of each RNA were bound in identical positions. The most favored site packed nucleotides 3 and 4 along the edge of the cavity that is demarcated by Lys-119 and Lys-159 (Fig. 1B). Regarding the second, third, and fourth nucleotides of the modeled bound mRNA, the phosphate-ribose backbone and not the bases interacted with the β-sheet of eIF4E. This mode of binding has been observed in the cocrystal structure of VP-39, a vaccinia virus protein that has cap-dependent 2′-*O*-methyltransferase activity, with an m^7G capped oligoribonucleotide which permits the protein to bind RNA in a sequence-non-specific manner [32,33]. The orientation of a bound RNA in VP-39 and that predicted for eIF4E is different from the RNA recognition motif described for RNPs that specifically bind U series RNAs [34,35]. RNPs contain solvent-exposed aromatic residues on the interior β-sheet, which stack with bases of the bound RNA in a manner that is not base specific. Such aromatic residues are not seen in the β-sheet region forming the RNA binding site of eIF4E. Instead, positively charged residues (Lys, Arg) are present on this surface, suggesting that it interacts with the phosphate backbone of a bound RNA.

Using the modeled mRNA and allowing flexibility of the C1–N9 bond of guanine bases and the chi1 and chi2 bonds of Lys-119, the hydrogen on C8 of the 5′-m^7G cap, of G2, and of G3 was 20 Å, 5 Å, and 5 Å away from the epsilon nitrogen of Lys-119, respectively. This suggests that Lys-119 could not cross-link with 8-N_3GTP bound in the m^7GDP cap site without extensive rearrangements of the protein structure, yet could readily cross-link with a N_3GDP bound in the second (or third) nucleotide binding site of the model with only slight shifts in the S4–H2 loop and the S5–6 loop (Fig. 1B). Such structural shifts were implied in the differences seen in the crystal structure of the S5–6 loop observed in the two different asymmetric units solved [1].

The location of the modeled mRNA binding site is consistent with the path of a capped mRNA bound to mammalian eIF4E and the solution structure of yeast eIF4E with m^7GpppA (Fig. 1B) [1,11]. The capped mRNA extends from Trp-56/Trp-102 (Trp-58/Trp-104 in yeast) and travels through the concave surface of the β-sheet. The fact that m^7GTP was able to specifically compete with photocross-linking of the 8-N_3GTP probe is most likely due to competition at the level of the 3′-phosphates rather than competition between the purine ring moieties [2]. Because of the 5′–5′ linkage of the mRNA cap, the phosphates of each NTP would be facing the

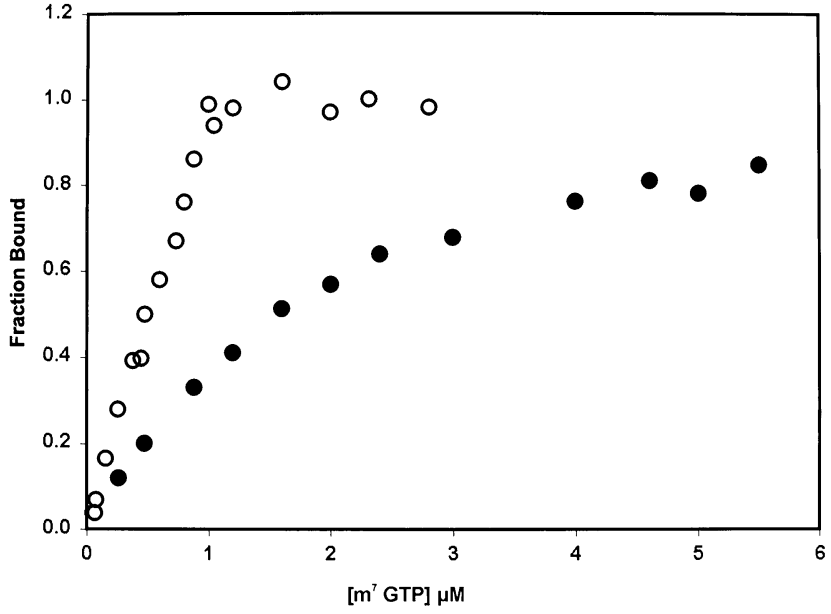

Fig. 3. Measurements of the fraction of protein bound as a function of m^7GTP concentrations were performed for wild-type eIF4E and K119A. All measurements were done in 20 mM HEPES-KOH (pH 7.6) and 1 mM DTT, at 23°C and at a protein concentration of 1 μM. An excitation wavelength of 289 nm was used to monitor the fluorescence intensity at 330 nm. The symbols represent (●) wild-type and (○) K119A eIF4E.

phosphates of 8-N_3GTP and would compete for the same binding site (Fig. 1B). Thus as the experiments showed, the photolabeling of 8-N_3GTP was most effectively inhibited by capped mRNA (95%), m^7GTP (84%), GTP (79%), and GDP (74%) while photolabeling was inhibited only slightly by GMP (27%) [2].

3.2. Expression and purification of eIF4E mutants

To further study the site identified by photoaffinity labeling, we mutagenized the S4–H2 loop. Four eIF4E mutants were produced with residues N118, K119, Q120, or Q121 mutated to alanine. Wild-type and mutants of eIF4E were expressed in *E. coli* and milligram quantities of proteins were purified (see Section 2). Analysis of the purified mutants of eIF4E by SDS–PAGE demonstrated greater than 90% purity (Fig. 2). The yields for both wild-type and mutant eIF4E were between 1 and 2 mg of purified protein per liter of *E. coli* culture. Characterization of the eIF4E mutants indicated that mutagenesis did not disrupt several functions. Mutant proteins with residues 118–121 changed to alanine were able to bind m^7GTP Sepharose and had circular dichroism spectra that were similar to wild-type eIF4E (data not shown). In addition, their ability to bind the translational repressor protein PHAS-I was not altered as determined by co-immunoprecipitating the two proteins with anti-eIF4E serum (not shown).

3.3. Affinity of eIF4E mutants for m^7GTP

The preparation of relatively large quantities of recombinant eIF4E mutants permitted their K_d of binding to the mRNA cap structure to be directly determined. Quantitation was performed by measuring the fluorescence quenching of intrinsic tryptophan residues in eIF4E upon m^7GTP binding at 25°C. The K_d value of recombinant wild-type eIF4E for m^7GTP was 1.2 μM and is similar to that reported for the native protein [29,31]. While Q121A had a K_d for m^7GTP that was similar to wild-type eIF4E (K_d of 1.1 and 1.2 μM, respectively), the N118A, K119A, and Q120A mutants all had significantly higher binding affinities with a K_d of < 0.30 μM for m^7GTP. Substituting residues in strand 4 of eIF4E with alanine produced no mutants with similar increases in their affinity for m^7GTP (not shown). The quenching curves for wild-type eIF4E and K119A are shown in Fig. 3. Furthermore, the N118A, K119A, and Q120A mutants of eIF4E did not show an ionic strength dependence for m^7GTP binding as is the case for wild-type eIF4E [29].

The interaction between eIF4E and mRNA caps is an essential and regulated step of gene expression. We provide evidence that specific mutations that are distant to the m^7GTP binding site of eIF4E can increase the affinity of m^7GTP binding. The N118A, K119A, and Q120A mutants of eIF4E provide novel examples of isoforms of eIF4E which have an affinity for m^7GTP that is up to one order of magnitude higher than wild-type eIF4E. All of these mutations are located in the S4–H2 loop. One possible explanation for the observed increased affinity for m^7GTP would be minor modifications in the position or orientation of the tryptophan residues, located in the S1–S2 (W56) and S3–S4 (W102) loops, which π–π stack with the m^7G moiety of mRNA [1,25]. It will be interesting to eventually determine if the mechanism(s) involved share similarities with or are different than those explaining the decreased affinity of mRNA cap binding that occurs when PML binds eIF4E [23,24]. Current efforts are being aimed at determining if the high affinity mutants of eIF4E may have practical use in improving methods of isolating mRNA with intact 5′-ends [36]. A better understanding of the reason for the increased affinity of these mutants for m^7GTP may permit eIF4E to be further engineered for specific purposes.

Acknowledgements: We thank A.E. Hodel for his suggestions in the comparison of the VP-39/m^7GDP cocrystal. This work was supported by NIH Grant CA63640 (C.H.H.). D.J.G. was supported by the National Science Foundation (MCB-0076344) and a PSC-CUNY Faculty Award. D.E.F. was supported by the National Science Foundation (pre-doctoral fellowship DGE-9553549), Glaxo-Wellcome Co. (Gertrude Elion Fellowship), and a Helen Samuels Schectman Scholarship.

References

[1] Marcotrigiano, J., Gingras, A.-C., Sonenberg, N. and Burley, S.K. (1997) Cell 89, 951–961.
[2] Friedland, D.E., Shoemaker, M.T., Xie, Y., Wang, Y., Hagedorn, C.H. and Goss, D.J. (1997) Protein Sci. 6, 125–131.
[3] Crew, J.P., Fuggle, S., Bicknell, R., Cranston, D.W., de Benedetti, A. and Harris, A.L. (2000) Br. J. Cancer 82, 161–166.
[4] Rousseau, D., Gingras, A.C., Pause, A. and Sonenberg, N. (1996) Oncogene 13, 2415–2420.
[5] Nathan, C.A., Carter, P., Liu, L., Li, B.D., Abreo, F., Tudor, A., Zimmer, S.G. and de Benedetti, A. (1997) Oncogene 15, 1087–1094.
[6] Donze, O., Jagus, R., Koromilas, A.E., Hershey, J.W. and Sonenberg, N. (1995) EMBO J. 14, 3828–3834.
[7] Yamanaka, S., Poksay, S., Arnold, K.S. and Innerarity, T.L. (1997) Genes Dev. 11, 321–333.
[8] Aktas, H., Fluckiger, R., Acosta, J.A., Savage, J.M., Palakurthi, S.S. and Halperin, J.A. (1998) Proc. Natl. Acad. Sci. USA 95, 8280–8285.
[9] Fraser, C.S., Pain, V.M. and Morley, S.J. (1999) J. Biol. Chem. 274, 196–204.
[10] Mazumder, B., Seshadri, V., Imataka, H., Sonenberg, N. and Fox, P.L. (2001) Mol. Cell Biol. 19, 6440–6449.
[11] McGuire, A.M., Matsuo, H. and Wagner, G. (1998) J. Biomol. NMR 12, 73–88.
[12] Matsuo, H., Li, H., McGuire, A.M., Fletcher, C.M., Gingras, A.C., Sonenberg, N. and Wagner, G. (1997) Nat. Struct. Biol. 4, 717–724.
[13] Sachs, A.B., Sarnow, P. and Hentze, M.W. (1997) Cell 89, 831–838.
[14] Kozak, M. (1992) Annu. Rev. Cell Biol. 8, 197–225.
[15] Sonenberg, N. and Gingras, A.C. (1998) Curr. Opin. Cell Biol. 10, 268–275.
[16] Rhoads, R.E. (1999) J. Biol. Chem. 274, 30337–30340.
[17] Donaldson, R.W., Hagedorn, C.H. and Cohen, S. (1991) J. Biol. Chem. 266, 3162–3166.
[18] Lazaris-Karatzas, A., Montine, K.S. and Sonenberg, N. (1990) Nature 345, 544–547.
[19] de Benedetti, A. and Rhoads, R.E. (1990) Proc. Natl. Acad. Sci. USA 87, 8212–8216.
[20] Lawrence Jr., J.C., Fadden, P., Haystead, T.A. and Lin, T.A. (1997) Adv. Enz. Regul. 37, 239–267.
[21] Stebbins-Boaz, B., Cao, Q., de Moor, C.H., Mendez, R. and Richter, J.D. (1999) Mol. Cell 4, 1017–1027.
[22] Morley, S.J., Jeffrey, I., Bushell, M., Pain, V.M. and Clemens, M.J. (2000) FEBS Lett. 477, 229–236.
[23] Cohen, N., Sharma, M., Kentsis, A., Perez, J.M., Strudwick, S. and Borden, K.L. (2001) EMBO J. 20, 4547–4559.
[24] Kentsis, A., Dwyer, E.C., Perez, J.M., Sharma, M., Chen, A., Pan, Z.Q. and Borden, K.L. (2001) J. Mol. Biol. 312, 609–623.
[25] Hsu, P.C., Hodel, M.R., Thomas, J.W., Taylor, L.J., Hagedorn, C.H. and Hodel, A.E. (2000) Biochemistry 39, 13730–13736.
[26] Shoichet, B.K. and Kuntz, I.D. (1993) Protein Eng. 6, 723–732.
[27] Hagedorn, C.H., Spivak-Kroizman, T., Friedland, D.E., Goss, D.J. and Xie, Y. (1997) Protein Expr. Purif. 9, 53–60.
[28] Haystead, T.A.J., Haystead, C.M.M., Hu, C., Lin, T.-A. and Lawrence Jr., J.C. (1994) J. Biol. Chem. 269, 23185–23191.

[29] Carberry, S.E., Rhoads, R.E. and Goss, D.J. (1989) Biochemistry 28, 8078–8083.
[30] Wang, Y., Sha, M., Ren, W.Y., van Heerden, A., Browning, K.S. and Goss, D.J. (1996) Biochim. Biophys. Acta 129, 207–213.
[31] Carberry, S.E., Darzynkiewicz, E., Stepinski, J., Tahara, S.M., Rhoads, R.E. and Goss, D.J. (1990) Biochemistry 29, 3337–3341.
[32] Hodel, A.E., Gershon, P.D. and Quiocho, F.A. (1998) Mol. Cell 1, 443–447.
[33] Hodel, A.E., Gershon, P.D., Shi, X., Wang, S.-M. and Quiocho, F.A. (1997) Nat. Struct. Biol. 4, 350–353.
[34] Kenan, D.J., Query, C.C. and Keene, J.D. (1991) Trends Biochem. Sci. 16, 214–220.
[35] Allain, F.H.-T., Howe, P.W.A., Neuhaus, D. and Varani, G. (1997) EMBO J. 16, 5764–5774.
[36] Edery, I., Chu, L.L., Sonenberg, N. and Pelletier, J. (1995) Mol. Cell. Biol. 15, 3363–3371.